

Damped Ly α Absorbing Galaxies At Low Redshifts $z \leq 1$ From Hierarchical Galaxy Formation Models

Katsuya Okoshi

National Astronomical Observatory, Mitaka, Tokyo 181-8588, Japan;

`okoshi.katsuya@nao.ac.jp`

and

Masahiro Nagashima

Department of Physics, University of Durham, South Road, Durham DH1 3LE, England

Department of Physics, Graduate School of Science, Kyoto University, Sakyo-ku, Kyoto 606-8502, Japan

ABSTRACT

We investigate Damped Ly α absorbing galaxies (DLA galaxies) at low redshifts $z \leq 1$ in the hierarchical structure formation scenario. In our previous paper, we showed that our model of galaxy formation can explain basic properties of Damped Ly α (DLA) systems such as the metallicity evolution and H I column density distribution. As a subsequent study, we focus on low-redshift DLA systems in detail to be compared with recent data of many characteristics and their relationships such as luminosities, H I column densities and sizes of galaxies with large H I column densities enough to produce DLA absorptions obtained by optical/radio observations. While it has been debated about what types of galaxies correspond to DLA systems, by using a theoretical model simultaneously treating with both DLA systems and galaxies, we clarify the nature of low-redshift galaxies producing DLA absorptions because observational data of such galaxies mainly at low redshifts are currently available. We find that our model well reproduces distributions of fundamental properties of DLA galaxies such as luminosities, column densities, impact parameters obtained by optical and near-infrared imagings. Our results suggest that DLA systems primarily consist of low luminosity galaxies with small impact parameters (typical radius ~ 3 kpc, surface brightness from 22 to 27 mag arcsec $^{-2}$) similar to low surface brightness (LSB) galaxies. In addition, we investigate selection biases arising from the faintness and from *the masking effect* which prevents us from identifying a DLA galaxy hidden or contaminated by a point spread function of a background

quasar. We find that the latter affects the distributions of DLA properties more seriously rather than the former, and that the observational data are well reproduced only when taking into account the masking effect. The missing rate of DLA galaxies by the masking effect attains 60 – 90% in the sample at redshift $0 \leq z \leq 1$ when an angular size limit is as small as 1 arcsec. Furthermore we find a tight correlation between H I mass and cross section of DLA galaxies, and also find that H I-rich galaxies with $M_{\text{HI}} \sim 10^9 M_{\odot}$ dominate DLA systems at $z \sim 0$. These features are entirely consistent with those from the Arecibo Dual-Beam Survey which is a blind 21 cm survey. Finally we discuss star formation rates, and find that they are typically about $10^{-2} M_{\odot} \text{ yr}^{-1}$ as low as those in LSB galaxies.

Subject headings: galaxies : formation - galaxies: evolution - quasars : absorption lines -radio lines: galaxies

1. Introduction

Numerous absorption lines found in the quasar spectra are one of few observational opportunities that provide us fruitful information on the physical state of the evolving universe. These absorption lines offer several advantages over emission lines. For example, the line features reflect the physical state of the astronomical objects and the intergalactic medium. Another advantage comes from the fact that absorption lines are free from observational limitations of the detection of absorbers caused by their faintness in photometric surveys.

Among those absorption line systems, damped Ly-alpha (DLA) systems would provide exceptional insights into exploring galaxy formation. DLA systems have been interpreted to arise from cold gas in galactic disks along lines of sight to quasars (Wolfe et al. 1986). So far some observational facts on DLA systems are obtained from detailed studies of quasar absorption spectra, for example, (1) the H I column densities are similar to those in our Galaxy, (2) most of them have low metallicities, $\sim 1/10 Z_{\odot}$ (e.g. Prochaska et al. 2003) and (3) the H I column density distributions are fitted by a single power law as well as those of the Ly α forest (e.g. Storrie-Lombardi & Wolfe 2000; Péroux et al. 2003). These facts suggest that DLA systems are galaxies in an early evolutionary stage. Therefore, it could be an interesting issue whether theoretical models of galaxy formation can consistently account for fundamental properties of DLA systems.

Furthermore, some low-redshift DLA systems can be also directly observed in recent photometric surveys. These samples provide a clue to revealing what types of intervening

galaxies arise DLA lines in quasar spectra, which are referred as ‘DLA galaxies’ hereafter. Such low-redshift DLA galaxies have been studied from both direct photometric images and spectroscopic follow-ups (e.g. Steidel et al. 1994, 1997; Lanzetta et al. 1997; Le Brun et al. 1997; Fynbo et al. 1999; Rao & Turnshek 1999; Turnshek et al. 2001; Bouché et al. 2001; Bowen, Tripp & Jenkins 2001; Warren et al. 2001; Møller et al. 2002; Rao et al. 2003; Chen & Lanzetta 2003; Schulte-Ladbeck et al. 2004; Møller, Fynbo & Fall 2004). The results of the searches suggest that DLA systems have a wide range of the morphology from dwarf galaxies to spirals and do not comprise a single population such as normal spiral galaxies. This picture is rather consistent with what is expected from the hierarchical structure formation scenario based on a cold dark matter (CDM) models because those predict that galaxies can span a mixture of their morphological types from dwarf to massive spiral galaxies. So it is clearly valuable to compare the observed properties of DLA galaxies with those predicted by theoretical models as a useful test of theories of galaxy formation.

Semi-analytic modeling has been applied with a view to deciphering the clues to the formation process of galaxies in the hierarchical clustering scenario. This approach takes into account merging histories of dark halos based on the power spectrum of the initial density fluctuation, and has successfully provided galaxy formation models for explaining observational properties of galaxies such as luminosity functions, the relation between H I gas mass fraction and luminosities, and so forth. It has some advantages over numerical hydrodynamical simulations. For example, it can clarify the effect of star formation or supernovae feedback on galaxy evolution even under simple recipes. Moreover, it does not also suffer from resolution limitations in numerical hydrodynamic simulations. This is important to study the formation process of small objects that are hardly resolved by numerical simulations. Therefore, it is valuable to apply this model for studying the evolution of DLA systems which tightly correlate with galaxies. So far, several semi-analytic models have been developed and provided interesting results for physical relations between DLA systems and galaxies (Kauffmann 1996; Somerville, Primack & Faber 2001; Maller et al. 2001, 2003; Okoshi et al. 2004, hereafter Paper I). In Paper I, we focused on the metallicity evolution and the H I column density distribution, and concluded that DLA systems primarily consist of dwarf and/or sub- L^* galaxies. As a subsequent study, this paper expands on these previous results to reveal the nature of low-redshift DLA systems by exploring typical properties of DLA galaxies obtained by recent observations. Here, the following advantages of this study should be addressed. (1) Our model can reproduce main properties of DLA systems, that is, the metallicity evolution and the H I column density distribution, (2) Our model incorporates with various effects in detecting DLA galaxies: cosmological dimming of the surface brightness, internal dust absorption and the observational bias caused by glare of quasars behind DLA galaxies along lines of sight. (3) Our model can also reproduce many

observational results of galaxy population such as luminosity functions and number counts (see Nagashima et al. 2001). This is the first theoretical study using a hierarchical galaxy formation model to explore photometric and radio properties of low-redshift DLA galaxies comprehensively enough to compare with the currently available observations.

In §2, we briefly describe our model. In §3, we show the results for various properties of DLA galaxies. In §4, we discuss selection biases for detection of DLA galaxies. In §5, we explore some possibilities to study the nature of DLA galaxies. We focus on the radio properties of DLA systems. We also discuss the star formation rates in DLA galaxies, which can be a good tracer for discerning what types of galaxies comprise the population of DLA systems. Finally we summarize our conclusions and discuss our results in comparison with other observations in §6.

2. Model

The semi-analytic model of galaxy formation used here is based on cold dark matter models in which, assuming a power spectrum of initial density fluctuations, dark halos emerge from the density fluctuations, cluster gravitationally, and merge together. Gas in dark halos cools and then forms stars. Such processes lead to the formation of galaxies which comprise gas and stars embedded in dark halos. After galaxies form, some galaxies grow up to massive ones like our Galaxy via merging processes. We apply this scenario to the study of the nature and formation of DLA systems in a framework of semi-analytic modeling. The semi-analytic model of galaxy formation used here is the same as the LC model described by Paper I, which well reproduces the observed number distributions and metallicity evolution of DLA systems. This model also well reproduces many aspects of observed properties of galaxies such as luminosity functions, cold gas mass fractions, disk sizes, and faint galaxy number counts in a Lambda-CDM model (Nagashima et al. 2001). We provide an outline of this model below.

The cosmological parameters we adopted are $\Omega_0 = 0.3$, $\Omega_\Lambda = 0.7$, $\Omega_b = 0.015h^{-2}$, $h = 0.7$ (where h is the Hubble parameter, $h = H_0/100\text{km s}^{-1} \text{Mpc}^{-1}$), and $\sigma_8 = 1$ that is the normalization of the power spectrum of density fluctuations given by Bardeen et al. (1986). The number density of dark halos at present is given by the Press-Schechter mass function (Press & Schechter 1974). The past merging history of each dark halo is realized by a Monte Carlo method proposed by Somerville & Kolatt (1999), which is based on an extended Press-Schechter formalism (Bond et al. 1991; Bower 1991; Lacey & Cole 1993). Only halos with circular velocities $V_{\text{circ}} \geq 40 \text{ km s}^{-1}$ are identified as isolated halos, and others are regarded as the diffuse accretion mass.

We assume that baryonic gas consists of two phases: cold and hot. The gas in a halo should be shock-heated to the virial temperature of the halo after the halo collapses. The heated gas is defined as hot gas in our model. A part of hot gas cools quickly by radiative cooling and falls to gaseous disks, which is defined as cold gas. The cold gas then becomes available for star formation. The star formation rate (SFR) is assumed as

$$\dot{M}_* = \frac{M_{\text{cold}}}{\tau_*}, \quad (1)$$

where M_* and M_{cold} are the masses in stars and cold gas, respectively, and τ_* is the timescale of star formation. We assume a star formation timescale independent of redshift as follows,

$$\tau_* = \tau_*^0 \left(\frac{V_{\text{circ}}}{300 \text{ km/s}} \right)^{\alpha_*}. \quad (2)$$

The free parameters τ_*^0 and α_* are chosen by matching the model prediction of cold gas mass fractions of spiral galaxies to observed one because those directly determine the gas consumption rate. Therefore, they should play an important role in determining the observable characteristics of DLA systems. As a result in Paper I, we have found that the above prescription of star formation with $(\tau_*^0, \alpha_*) = (1.5 \text{ Gyr}, -2)$ successfully reproduces both metallicity evolution and H I column density distributions of observed DLA systems (see Figures 1 and 3 in Paper I). Thus, we adopt these values in this study. From the estimated SFR, luminosities of galaxies are computed by using simple stellar populations given by Kodama & Arimoto (1997). We also include a supernova feedback process and merging process of galaxies. The details are described in Paper I.

Finally, we address DLA systems in our model. We simply assume that all DLA systems have gaseous disks which are face-on to an observer because the inclination effect hardly affects the column density distributions (see Figure 4 in Paper I). Here, the radial distribution of the H I column density follows an exponential profile with an effective radius of a gaseous disk, r_e . It is assumed to be $r_e = r_0(1+z)$ where r_0 is a radius provided by the specific angular momentum conservation of cooling hot gas. We also assume that the dimensionless spin parameter has a log-normal distribution with the average 0.06 and the logarithmic variance 0.6. The central column density N_0 is given by $N_0 = M_{\text{cold}}/(2\pi\mu m_{\text{H}}r_e^2)$, where m_{H} is the mass of a hydrogen atom and $\mu(= 1.3)$ is the mean molecular weight. The size of a DLA system is defined by the radius R at which $N_{\text{HI}} = 10^{20} \text{ cm}^{-2}$. For each system, we take the column density averaged over radius within R . The above definition of DLA systems is the same as in Paper I.

We assume that cold gas in DLA systems is neutral. This would be justified as follows. The H I column density of DLA systems exceeds about 10^{20} cm^{-2} , which means that the

cold gas is optically thick. So the ionization fraction averaged over the whole disk should be very small even if the UV background radiation exists around DLA systems. Prochaska & Wolfe (1996) calculated the ionization fraction in DLA systems taking into account radiation transfer, assuming a UV background intensity corresponding to that at $z \sim 2 - 3$, which probably be higher than at $z \lesssim 1$. When a DLA system is a uniform gas layer with a number density $n = 0.1 \text{ cm}^{-3}$, which is similar to that of typical DLA systems in our model, they found the ionization fraction $x(= n_e/n) < 0.1$. It could be also possible that far UV radiation emitted from internal OB stars ionizes the hydrogen atoms in disks. Radio observations of ionized gas in our Galactic disk, however, have revealed that the mass ratio of H II to H I gases is about 0.01, and that the filling factor of H I gas is less than 0.1 (Osterbrock 1989). We consider that the ionization fraction in DLA systems should be smaller than that in our Galaxy because ionizing photons are expected to be less than in our Galaxy, inferred from smaller SFRs in DLA systems. This feature has been also confirmed by recent measurements of the Al III abundance in DLA systems (Vladilo et al. 2001). The Al III abundance is a good tracer for estimating the intensity of ionizing UV radiation because the production of Al III requires UV photons. They concluded that cold gas in DLA systems is almost neutral from the observed small abundance of Al III. Therefore, it is reasonable to assume that cold gas in DLA systems is neutral.

3. DLA Galaxy Properties at low redshift

As shown in Paper I, our model has a good ability to reproduce various properties not only of galaxies both at high and low redshifts but of DLA systems, particularly the observed distributions in the H I column density and the metallicity evolution. Here we present various properties of DLA galaxies at redshift $0 \leq z \leq 1$. Recently, Rao et al. (2003) compiled observational data of 14 DLA systems, including new identified ones, at $0 \leq z \leq 1$ and showed distributions of their properties (luminosities, neutral hydrogen column densities, impact parameters and number distributions). Their conclusion is that low-luminosity dwarf galaxies with small impact parameters dominate their compiled sample. Below we compare statistical properties of DLA systems in our model with the observations. Note that, in our calculation, the total number of model DLA galaxies is very large, for example, $\sim 8 \times 10^3$ and the covering comoving volume is $\sim 2 \times 10^9 \text{ Mpc}^3$ at redshift $z = 0$, which are statistically large enough to investigate the DLA properties. Note also that when presenting averaged values over redshifts, the comoving volume element dV/dz is taken into account.

Following the presentation of the observational data by Rao et al. (2003), Figure 1 shows distributions of properties of DLA galaxies about luminosities in B -band relative to

L^* , which corresponds to $M_B = -20.9$ mag (Rao et al. 2003), neutral hydrogen column densities N_{HI} and radii b . Figure 1(a) shows the luminosity evolution from $z = 1$ to present. We find that average luminosities predicted by our model are broadly consistent with those of some observed DLA galaxies at low redshifts, while some are brighter than our results. As shown in Paper I, our model predicts that the average circular velocities of dark halos hosting DLA systems increase toward low redshift as merging proceeds, and that the average attains $V_{\text{circ}} \sim 90 \text{ km s}^{-1}$ at redshift $z = 0$ (see Figure 8 in Paper I). The luminosities also increase gradually as the star formation proceeds, and the average luminosity is $L \sim 2 \times 10^9 L_{\odot} \sim 0.05 L^*$ at present (see Figure 10 in Paper I), which are fainter than those of some normal spirals, $\sim L^*$. Thus our model apparently predict the average luminosities of DLA galaxies lower than the observations, which include some L_* -galaxies as shown in Figure 1(a), unless any relevant selection biases as discussed in next section are taken into account.

In Figures 1(b) and (c), our results show that DLA galaxies typically have neutral hydrogen column densities $N_{\text{HI}} \sim 10^{20.6} \text{ cm}^{-2}$ and radii $b \sim 3 \text{ kpc}$ (see also panels i and j), and their evolution is very moderate at $z \lesssim 1$. In Figure 1(c), it appears that the mean sizes are generally smaller than the observations. Because the radial sizes in our calculation provide upper limits of impact parameters, our model seems to underpredict the sizes of DLA systems. Figure 1(d) depicts the number fraction of DLA galaxies as a function of redshift. Our result shows that the number increases toward higher redshift. This matches the observational trend of the redshift distribution of *absorption line* systems, dN/dz , that their number increases up to $z \sim 5$ (e.g. Storrie-Lombardi & Wolfe 2000; Prochaska & Herbert-Fort 2004). Note that the number of DLA galaxies in panel(d) is not identical to dN/dz . The former is weighted by the comoving volume element dV/dz and the latter by the cross section of DLA systems.

Figures 1(e) and (f) present the mean column density and impact parameter as a function of luminosity. DLA galaxies with lower luminosities tend to have smaller impact parameters, while *mean* column densities depend very weakly on the luminosities for $L/L^* \gtrsim 0.1$. Note that Figure 1(f) indicates that some bright galaxies have large sizes with radii $b \gtrsim 10 \text{ kpc}$ while the mean is $\sim 3 \text{ kpc}$. Our result also suggests that DLA galaxies with large b ($\gtrsim 20 \text{ kpc}$) should be identified as L^* spirals. We thus emphasize that luminous galaxies ($\gtrsim L^*$) arise damped $\text{Ly}\alpha$ absorptions although the number fraction is much lower than that of the dominant population ($L \lesssim 0.1 L^*$). This is in agreement with the observational fact that DLA systems have a wide range of morphology from dwarf galaxies to bright spirals.

We also show how the extent of neutral gas around DLA galaxies scales with the column densities in Figure 1(h). The relation between b and $\log N_{\text{HI}}$ suggests that most of DLA systems have impact parameters smaller than 10 kpc . This figure also shows a trend

that DLA galaxies with large N_{HI} have small sizes, similar to the observation. Our model, however, seems to underpredict the size as shown in Figure 1(c). This reason is discussed in next section.

From the above results, it is suggested that DLA systems mainly comprise dwarf galaxies with small sizes. This is consistent with some trends emerging in the observation (Rao et al. 2003). Nevertheless, some observational data show that DLA galaxies are likely to be brighter and observed at impact parameters larger than our results although the available sample is still small in the observations. These differences might be also alleviated if some selection biases exist such that bright galaxies should likely be observed with large impact parameters, in other words, most of optical counterparts of DLA systems are hardly identified because of the faintness. In general, the identification of DLA galaxies among a large number of the candidates requires both photometric images and spectroscopic follow-ups. It is often extremely difficult to pick out their candidates and/or to identify them accurately. This is partly because they have low surface brightness and partly because the candidates exist in close proximity to a quasar line of sight. Below we investigate how such selection biases affect the distributions of DLA-galaxy properties discussed here.

4. Selection bias

4.1. Surface Brightness Limit

Firstly, we focus on surface brightness distributions of DLA galaxies at redshift $0 \leq z \leq 1$ because detection limits are usually determined by a surface brightness. Figure 2 shows the B -band central surface brightness μ of DLA galaxies. Figure 2(a) depicts the evolution of their mean surface brightness. We find that the surface brightness becomes fainter toward higher redshift and that the mean surface brightnesses are ~ 22 mag arcsec $^{-2}$ at $z \sim 0$ and ~ 27 mag arcsec $^{-2}$ at $z \sim 1$. The evolution of surface brightnesses arises from both the luminosity evolution and cosmological dimming.

We also show distributions of central surface brightness averaged over $0 \leq z \leq 1$ weighted by the comoving volume element against luminosities, column densities and sizes, in Figures 2 (b)-(d), respectively. Our results suggest that the surface brightness does not apparently depend on both the luminosity for $L/L^* \gtrsim 0.1$ and the radius but the column density.

Figure 3 shows the number fractions as a function of μ at redshifts $z = 0, 0.5$ and 1 . These results clearly represent that DLA galaxies become brighter toward low redshift and the mean central surface brightness does by about 5 mag from $z = 1$ to 0 . We also find the

average surface brightness $\mu \sim 25 \text{ mag arcsec}^{-2}$ at $0 \leq z \leq 1$.

Very low surface brightness DLA galaxies computed here are not expected to be detected because of the faintness below the detection limit. Although the limit depends on the quasar fields, for example, Rao et al. (2003) set their 3σ limiting surface brightnesses of around $25 \text{ mag arcsec}^{-2}$ (Table 2 in their paper). According to the surface brightness limit, we pick out DLA systems with $\mu \leq 25 \text{ mag arcsec}^{-2}$ and show distributions of their properties in Figures 4, in which the number fractions shown in bottom panels are defined as the ratios the number of DLA galaxies per bin to that of DLA galaxies which fulfill the selection criteria. Our results show that most distributions are very similar to those without the limit in Figure 1, while the mean N_{HI} becomes larger particularly at high redshift $z \sim 1$ and the number fraction in N_{HI} (panel i) shows that DLA galaxies apparently decrease in low $N_{\text{HI}} \lesssim 10^{21} \text{ cm}^{-2}$. These tendencies stem from the following reasons. In Figures 2, we found that high surface brightness galaxies have gaseous disks with high N_{HI} . In other words, the surface brightness is strongly correlated with the column density. At high redshifts, the low surface brightness galaxies dominate the population of DLA systems. Therefore, picking out only the high surface brightness systems arises the increase of the mean column densities at high redshifts. In contrast, the surface brightness is not significantly correlated with the luminosity and the size. This causes the results that the distributions of L and b are still similar to those without the surface brightness limit. Therefore, we find that this selection effect does not account for the observed distributions of DLA galaxy properties when the limit is as low as $\mu \sim 25 \text{ mag arcsec}^{-2}$.

4.2. Angular Size Limit

Second, we focus on a selection effect caused by angular sizes of DLA galaxies. Identification of a DLA galaxy requires accurate determination of its redshift which must be identical to that of a DLA system as a possible counterpart. If a DLA galaxy is compact and/or very close to a quasar line of sight, it often happens that the image is blended or hidden in the point spread function (PSF) of the background quasar. Even after subtracting the PSF from the blended image, noisy residuals often remain so that any information cannot be extracted within the radius of the circle enclosed by the PSF. *If a galaxy that gives arise to damped Ly α absorption is small and comparable to the size of the PSF*, it is more likely to arise this difficulty because the DLA galaxy is contaminated or hidden by the PSF. Even when the size is $\sim 1 \text{ arcsec}$, it corresponds to the scale at most $\sim 6 \text{ kpc}$ at $z = 0.5$ and $\sim 8 \text{ kpc}$ at $z = 1$ in the cosmological model adopted here. This selection effect, which is called the ‘masking effect’ hereafter, can be serious because DLA galaxies are expected to be very

compact, about 3kpc on average in our model.

Figure 5 presents the distributions of DLA galaxies as a function of the angular radius θ at $z = 0.1$ (*dotted line*), 0.5 (*dashed line*), and 1 (*solid line*), respectively. The number fraction in large θ decreases toward high redshift while the physical size of DLA galaxies apparently shows no evolution [see Figure 1(c)]. Thus, the evolution of the number distribution with redshift should be caused just by the distance varying which directly affects the angular size.

In our model, 60 – 90% of DLA systems have small angular sizes less than 1 arcsec. The limits of angular sizes caused by the PSF are usually different in observed images by images. In most observations, however, the limiting angular sizes are likely to be larger than 1 arcsec. Here, we set the angular size limit $\theta_{\text{th}} = 1$ arcsec and assume that DLA systems with angular sizes smaller than 1 arcsec are not precisely resolved or identified as DLA galaxies by the masking effect.

Taking into account this selection bias in addition to the surface brightness limit $\mu_{\text{th}} = 25$ mag arcsec $^{-2}$, we calculate distributions of DLA galaxies with angular sizes larger than 1 arcsec. The results are presented in Figure 6. We find that, at high redshifts, DLA systems with large sizes mainly contribute to optically observable DLA galaxies because the physical size corresponding to $\theta = 1$ arcsec increases toward high redshifts. This is confirmed by the result for the evolution of their sizes in Figure 6(c) in which the averages are larger than those in Figure 1(c) at $z \gtrsim 0.5$. Figure 6(c) suggests that DLA galaxies with large radii, ~ 10 kpc, obviously increase at redshift $z \gtrsim 0.5$ under the masking effect (cf. Figure 1(c)). It also appears that the number fraction of large b systems averaged over $0 \leq z \leq 1$ increases as shown in Figure 6(j) in comparison with Figure 1(j). The masking effect evidently causes better agreement with the observational data of the impact parameters particularly for large b [Figures 6(c) and (h)]. Figure 6(a) presents that this bias also affects the apparent evolution of the luminosity of observed DLA galaxies. The luminosities agree better with the observations in Figure 6(a) by taking into account the masking effect. This is because most of large DLA systems, which are dominant at high redshift, are bright as shown in Figure 6(f). Figure 6(d) shows that the redshift distribution of DLA galaxies exhibits a trend similar to that in Figure 1(d) for a model without the selection effects, while the number evolution becomes milder.

Figure 6 is one of the main results of this study, that is, it shows that the selection biases, particularly the masking effect, are very important when we interpret the observed results of DLA galaxies, and that the biases lead to much better agreement with the observations. This suggests that bright DLA galaxies are not representative of the entire population of galaxies producing damped Ly α absorptions because the masking effect makes difficult to identify faint and small galaxies as DLA galaxies.

To evaluate the masking effect on the luminosity more precisely, we vary the limit of angular size θ_{th} . Figure 7 shows the results for $\theta_{\text{th}} = 1, 2$ and 3 arcsec, respectively. The large θ_{th} produces better agreement with the luminous DLA galaxies. Because the large θ_{th} causes faint galaxies not to be identified as DLA galaxies statistically, our results show that the average luminosity increases and matches better with the observations.

We have shown that the masking effect should be taken seriously to the identification of DLA galaxies at high redshift although the limits depend on quasar fields. Our model also predicts that the missing rate of DLA galaxies by the masking effect attains 60-90 % in observations if the observable angular size is as small as 1 arcsec and if compact galaxies, $\lesssim 3$ kpc, contribute significantly to the population of DLA systems.

5. Predicted Properties & Implications

5.1. Some Properties Expected by Radio Observations

Here, we explore another way to studying DLA galaxies to avoid the selection biases. Are there any methods to identify galaxies producing damped Ly α absorptions apart from the masking effect? It is expected that radio surveys can detect this kind of galaxies at low redshift if they have H I column densities as large as those measured in DLA systems. We focus on the H I mass in DLA systems which correlates with observational properties in radio observations. The cross section of radio sources also provides a useful clue to studying the distribution of H I gas in the gaseous disk. First, a relation between H I masses and sizes in DLA systems is plotted as a solid line with 1σ error bars in Figure 8(a). We find that the logarithmic cross section, $\log \sigma$, is linearly proportional to the logarithmic H I mass, $\log M_{\text{HI}}$, i.e., $\sigma \propto M_{\text{HI}}^\alpha$. The relation is fitted by averaged least-squares and we find that the slope α is 0.97 ± 0.01 in the range of H I mass $10^{6.5} \leq M_{\text{HI}}/M_\odot \leq 10^{10.5}$.

Recently, Rosenberg & Schneider (2003) observed local H I-rich galaxies identified by a blind 21 cm survey: the Arecibo Dual-Beam Survey (ADBS). The ADBS sample consists of approximately 260 galaxies. They focused on the H I-selected galaxies which have H I column densities comparable to those in DLA systems. If a bright quasar existed behind them, such H I-selected galaxies should give rise to damped Ly α absorption in the quasar spectrum. Including other data provided by different observations, they found a correlation between the cross section and the H I mass such as $\log \sigma \propto \log M_{\text{HI}}$. The range of the observational data spreads within the dashed box region presented in Figure 8(a), which spans a wide range of masses $10^{6.5} \lesssim M_{\text{HI}}/M_\odot \lesssim 10^{10.5}$. The slope of the relation is estimated as 1.004 ± 0.021 in the sample. We find that this slope is entirely consistent with our results. The predicted

cross-sections are also within the range of the observational data. One might consider that the observed cross sections are somewhat larger than our results. The blind 21 cm emission-line survey has typical resolutions $\sim 10\text{--}60$ arcsec which are lower than those in photometric surveys. Such low resolutions may systematically lead to overestimates in the sizes of small galaxies.

We also show the averaged cross-section of DLA systems at $0 \leq z \leq 1$ as a dotted line. The slope is almost identical with that of the relation at $z = 0$ (solid line) because both the cross sections and the H I masses are almost constant against redshift [see Figure 1(c) and Figure 7 in Paper I]. We thus predict that the relation at high redshifts would be almost identical to that at $z = 0$. Figure 8(b) shows the number fraction in H I mass. As already discussed in Paper I, we find that the average of H I mass is about $10^9 M_\odot$ at $0 \leq z \leq 1$ in our model. This result agrees the observational feature that DLA galaxies are dominated by those with H I masses near $10^9 M_\odot$ (Rosenberg & Schneider 2003).

We put emphasis on the facts, first, that *the tight relation between the H I mass and the cross section is found in our model similar to the radio observations*, and second, that *our results are also consistent with the properties obtained by the radio observations in the whole observed range of H I mass*. We will extensively discuss the properties of the H I-selected galaxies in a separate paper.

5.2. Star Formation Rates

Star formation rates (SFRs) provide an important clue to understanding DLA galaxies. Figures 9 present the number fractions as a function of both SFR and SFR per unit area in DLA galaxies at $z = 0$ and 1, respectively. The SFR per unit area is simply estimated as SFR divided by the disk area. All galaxies are simply assumed to be face-on to us when computing the area because the effects of the inclination are negligible (see Figure 4 in Paper I). We here discard spheroidal galaxies because they have much less amount of H I gas than spirals and then much lower SFRs. This assumption is suitable for calculating the SFR per unit area.

In Figure 9 (a), we find that DLA galaxies have SFRs which widely ranges from 10^{-6} to $10^2 M_\odot \text{ yr}^{-1}$. At $z = 1$, the distribution of SFRs has a large variance and a long tail toward low SFRs $\lesssim 10^{-2} M_\odot \text{ yr}^{-1}$, while the variance at $z = 0$ is smaller than that at $z = 1$. Because less massive galaxies become dominant at high redshift (Figure 8 in Paper I) and they have long timescales of star formation, galaxies with low SFRs increases toward high redshift. We also find that the mean SFRs are $\sim 10^{-2} M_\odot \text{ yr}^{-1}$ at $0 \leq z \leq 1$. In Figure 9

(b), the distributions of SFRs per unit area at $z = 0$ and 1 are quite similar to each other with the mean values $\sim 10^{-2.8} \text{ M}_\odot \text{ yr}^{-1} \text{ kpc}^{-2}$.

Figure 10 shows various distributions of SFRs. We plot the correlations of SFRs with redshifts, luminosities, H I column densities, sizes and surface brightnesses. Figure 10(a) shows the redshift evolution of SFRs. This indicates that the SFRs of DLA systems are $\sim 10^{-2} \text{ M}_\odot \text{ yr}^{-1}$ at $z = 0 - 1$ and the evolution is quite moderate similarly to the stellar mass evolution (see Figure 7 in Paper I). It appears that the variances of SFRs decrease toward low redshift as also shown in Figure 9(a). Figures 10(b) depicts the relation between SFRs and luminosities. Clearly, brighter galaxies have higher SFRs. For example, DLA galaxies brighter than $L/L^* \sim 0.5$ have SFRs larger than $\sim 10 \text{ M}_\odot \text{ yr}^{-1}$ while the mean SFR is much lower, $\sim 10^{-2} \text{ M}_\odot \text{ yr}^{-1}$. It is also noticeable that DLA systems with high N_{HI} , large b and high (small value of) μ have larger SFRs in Figures 10(c),(d) and (e).

Consequently, our results imply that DLA galaxies have wide-ranged values of SFRs. In observational studies, SFRs in various types of galaxies have been derived and discussed by various authors. Measurements of SFRs give the most likely value of $\sim 3 \text{ M}_\odot \text{ yr}^{-1}$ for our Galaxy (Cox 2000). Petrosian et al. (1997) reported that SFRs of local blue compact galaxies are $\sim 0.3 - 0.5 \text{ M}_\odot \text{ yr}^{-1}$. SFRs of LSB galaxies estimated by van den Hoek et al. (2000) are about $0.03 - 0.2 \text{ M}_\odot \text{ yr}^{-1}$, using an empirical relation between H α and I -band surface brightnesses in galactic disks. For dwarf and LSB galaxies, van Zee (2001) compiled their observational characteristics and estimated the SFRs using optical images in UBV and H α passbands. The SFRs widely span at least 4 orders of magnitude, $\sim 10^{-5} - 10^{-1} \text{ M}_\odot \text{ yr}^{-1}$. The wide-ranged SFRs are broadly consistent with those predicted by our model. In this sample, the galaxies have central surface brightnesses between 20.5 and 25 mag arcsec $^{-1}$ and scale lengths of the disk from about 0.2 to 4.3 kpc. These properties are quite similar to those of DLA systems at $z \sim 0$ in our model. Bowen, Tripp & Jenkins (2001) found a nearby DLA galaxy (SBS1543+593) at $z = 0.009$ from photometric images obtained by a ground-based telescope and *Hubble Space Telescope* (*HST*). Because this DLA system is the closest to us, it is expected to provide some clues to revealing the various properties of DLA galaxies. Recently, Schulte-Ladbeck et al. (2004) reported a more detailed study of this galaxy and found that this has typical properties of LSB galaxies: the central surface brightness $\mu_B(0) = 22.8 \pm 0.3 \text{ mag arcsec}^{-2}$ and the SFR $\sim 0.006 \text{ M}_\odot \text{ yr}^{-1}$. These properties also agree with those in our model. Together with these observational facts, our result leads to a conclusion that DLA systems mainly comprise dwarf galaxies in which the SFRs are low comparable to those in LSB galaxies.

If DLA galaxies are faint and compact, it happens that most of the stellar counterparts cannot be detected by selection effects, which would prevent from estimating the SFRs

accurately by using emission lines. Absorption lines potentially provide us useful information on SFRs even if DLA galaxies are faint and compact. Recently, Wolfe, Prochaska, & Gawiser (2003a,b) successfully estimated the SFRs per unit area of about 30 galaxies at $z \gtrsim 2$ by a new method using C II* λ 1335.7 absorption line. They inferred the SFRs per unit area from the heating rate by far-ultraviolet radiation from massive stars under the assumption that the heating rate is equal to the rate of cooling by C II* line emission. Generally, the cold gas consists of two-phase media comprising a cold neutral medium (CNM) and a warm neutral medium (WNM). These media can stably exist in pressure equilibrium under some conditions which are determined by a thermal balance of the two phases (e.g. McKee & Ostriker 1977; Wolfire et al. 1995). For example, Wolfire et al. (1995) investigated the stable condition of the CNM and the WNM in the interstellar medium (ISM). They found that neutral gas exists in two stable phases, the CNM with typical temperature $T \sim 10^2$ K and a typical number density $n \sim 0.1 \text{ cm}^{-3}$, and the WNM with $T \sim 8000$ K and $n \sim 10 \text{ cm}^{-3}$. Wolfe, Prochaska & Gawiser (2003a) showed stable conditions of the CNM and the WNM in DLA systems similar to those in the ISM of the Milky Way. In our model at present stage, we assume that disk gas comprises uniformly one-phase medium for simplicity. When the disk gas is uniformly distributed throughout plane-parallel disks with radius $r \sim 3 \text{ kpc}$ and scale-height $h \sim 0.1 \text{ kpc}$, the typical number density is $n \sim 0.1(N_{\text{HI}}/10^{20.5} \text{ cm}^{-2})(h/0.1 \text{ kpc})^{-1} \text{ cm}^{-3}$. In a low-density medium ($n \lesssim 0.1 \text{ cm}^{-3}$), cosmic rays are a dominant source of heating and ionization (Wolfe, Prochaska & Gawiser 2003a). Assuming that the ionization rate by cosmic rays is proportional to the star formation rate, the ionization fraction depends on the star formation rate in addition to the number density and temperature. The physical conditions typically predicted by our model, $N_{\text{HI}} \sim 10^{20.5} \text{ cm}^{-2}$, the SFR per unit area $\sim 10^{-2.8} \text{ M}_{\odot} \text{ yr}^{-1} \text{ kpc}^{-2}$, and $n \sim 0.1 \text{ cm}^{-3}$, would result in the ionization fraction $x(= n_e/n)$ less than 0.1 (Wolfire et al. 1995; Wolfe, Prochaska & Gawiser 2003a), and suggests that the disk gas in our calculation roughly corresponds to the WNM for two-phase model. Wolfe, Prochaska & Gawiser (2003a) estimated the SFRs $\sim 10^{-3} - 10^{-2} \text{ M}_{\odot} \text{ yr}^{-1} \text{ kpc}^{-2}$ for DLA systems in case that C II* absorption occurs in the CNM, and $\sim 10^{-2} - 10^{-1} \text{ M}_{\odot} \text{ yr}^{-1} \text{ kpc}^{-2}$ for DLA systems in case that C II* absorption occurs in the WNM. Interestingly, the former SFRs agree well with those in our model. This might imply that C II* absorption occurs in the CNM at $z \gtrsim 2$ if the evolution of SFRs are moderate against redshift. It is also possible that the SFRs decrease toward low redshift ($z < 2$) in the WNM in which C II* absorption arises. Indeed, since we assume that the gas is uniformly distributed in the disk, our modeling for disk gas has not reached a crucial stage to compare our results with the estimated SFRs precisely. It would be valuable to investigate the evolution of multi-phase structure in DLA systems in a subsequent study. Recent hydrodynamical simulations have estimated SFRs of DLA systems. For example, using SPH simulation, Nagamine, Springel & Hernquist (2004) found that simulated DLA systems have SFRs per unit area as low as $\sim 10^{-3} - 10^{-2} \text{ M}_{\odot} \text{ yr}^{-1}$

kpc^{-2} . Their results should be suggestive to recognize that the simulated SFRs are consistent with our results. We should note that, however, their simulation has several limitations such as numerical resolutions, the narrow range of parameters related with star formation and supernova feedback, and so on, and also that they predicted about an order of magnitude higher metallicities of DLA systems than observed values.

Figure 11 shows the SFR per unit area as a function of the H I column density at redshifts $z = 0$ and 1 in comparison with the Kennicutt law, which is an empirical relation between the SFR surface density and the H I column density of local galaxies provided by Kennicutt (1998),

SFR surface density

$$= (2.5 \pm 0.7) \times 10^{-4} \left(\frac{N_{\text{HI}}}{1.25 \times 10^{20} \text{cm}^{-2}} \right)^{1.4 \pm 0.15} \text{M}_{\odot} \text{yr}^{-1} \text{kpc}^{-2}. \quad (3)$$

This relation is also represented in Figure 11 by the shaded region. We find that our SFRs broadly follow the Kennicutt law. In other studies, this trend is also emerged at redshift $z \gtrsim 2$ (Wolfe, Prochaska & Gawiser 2003a,b). In a numerical simulation, Nagamine, Springel & Hernquist (2004), furthermore, confirmed this tendency which seems to be independent of the strength of galactic winds. In addition with our results, these suggest that the SFRs follow the Kennicutt law at both low and high redshifts. This implies that the evolution of SFRs in DLA systems should be very moderate against redshift. Including other fundamental properties such as luminosities and sizes at high redshift, the SFR evolution at $z > 1$ will be also presented and discussed in a subsequent paper.

5.3. Sizes and H I column density distributions of DLA galaxies

Finally, we examine how the masking effect changes other properties of DLA galaxies. First, Figure 12 shows the radial size b as a function of B -band absolute magnitude brighter than $M_B \sim -17$ mag. Our result shows a trend that bright DLA galaxies are likely to be observed with large impact parameters. The mean radial size is apparently larger than the observational data because the radial size provides an upper limit of impact parameters. This scaling relation is fitted by averaged least-squares, $b \propto M_B^{\alpha}$, and we find the slope $\alpha = -0.18 \pm 0.02$ in the range of magnitude $-21 \leq M_B \leq -16.5$ mag. Taking into account the masking effect, we also show the $b - M_B$ relation as the dashed line in this figure. It is also evident that the masking effect with $\theta_{\text{th}} = 1$ arcsec hardly changes the slope for bright

galaxies because the masking effect reduces the number of only compact and faint galaxies. Recently, Chen & Lanzetta (2003) observationally found a scaling relation between the H I-disk size R and the B -band luminosity L_B of DLA galaxies, $R \propto L_B^\beta$ with $\beta = 0.26_{-0.06}^{+0.24}$. This relation is also plotted as the dotted line in Figure 12. We find that the scaling relation is consistent with our predicted one within 1σ scatters. For example, our relation has the indices $\beta = 0.35 \pm 0.02$ and 0.45 ± 0.01 with and without the masking effect, respectively. Thus the tight relationship between the radial size and the magnitude found in our model, which suggests that brighter galaxies are larger, is consistent with the observations.

Second, we calculate a neutral hydrogen column-density distribution of *DLA galaxies* taking into account the masking effect. Figure 13 shows the column density distribution at $z = 1$. The data points are taken from Storrie-Lombardi & Wolfe (2000)¹. We also take additional data reported by Rao & Turnshek (2000) which include a sample at low redshift $\langle z \rangle \sim 0.8$. In Paper I (Figures 3 and 5), we reproduced the column density distribution of DLA systems especially for low-redshift ones. In Figure 13, the solid and dashed lines indicate the distributions of DLA galaxies with and without the masking effect, respectively. The masking effect is the most significant at $z = 1$ because an angular size of a constant physical size approaches a minimum around $z = 1$. Therefore, this effect reduces the number of DLA galaxies over the whole range of column density. Even if $\theta_{\text{th}} = 1$ arcsec, we find that the column density distributions can be still consistent with the observational data (dashed line in Figure 13). We thus predict that optically-selected DLA galaxies also have the column density distribution similar to that of all Damped Ly α absorbers even if the selection effect exists.

6. Conclusions and Discussion

We have investigated damped Ly α absorbing galaxies at redshifts $0 \leq z \leq 1$ in the hierarchical structure formation scenario using a semi-analytic galaxy formation model. In the previous study (Okoshi et al. 2004), we found that our model can reproduce many fundamental properties of DLA systems such as the metallicity evolution, the column density distribution and the mass density of cold gas in addition to those of local galaxies (Nagashima et al. 2001). In this paper, we have focused our attention on their host galaxies that give arise to damped Ly α absorption at $0 \leq z \leq 1$ and use the model to calculate the observable properties. The main conclusions are the followings:

¹We adjust the data points for the cosmological model (LCDM) adopted here.

1. Most of DLA galaxies producing damped Ly α absorption lines in quasar spectra are faint and compact. Their typical size is ~ 3 kpc, and the mean surface brightnesses are ~ 22 mag arcsec $^{-2}$ at $z \sim 0$ and ~ 27 mag arcsec $^{-2}$ at $z \sim 1$, respectively. Some selection biases are required for those to have fundamental properties consistent with those of DLA galaxies observed in optical and near-infrared images (Rao et al. 2003).
2. Two selection biases were studied here. First is a bias caused by low surface-brightness galaxies. A typical limit of surface brightness in observations, $\mu_{\text{th}} = 25$ mag arcsec $^{-2}$, has a negligible effect. Second is *the masking effect*, under which only large DLA galaxies are detectable because small ones must reside in close proximity to a quasar line of sight where the quasar PSF dominates. Considering a typical masking angular size $\theta_{\text{th}} = 1$ arcsec, this effect is significant and makes the distributions of fundamental properties of DLA galaxies much better agree with the observations.
3. The missing rate of DLA galaxies by the masking effect attains 60 – 90 % if low-luminosity galaxies with small impact parameters (~ 3 kpc) significantly contribute to the population of DLA systems.
4. A tight relation between the H I mass and the cross section was confirmed in DLA systems. We also found that H I-rich galaxies with $10^9 M_{\odot}$ mainly contribute to the population of DLA systems at $z \sim 0$. These results are entirely consistent with the properties of H I-selected galaxies in a radio survey (*the Arecibo Dual-Beam Survey*, Rosenberg & Schneider 2003). The investigations by such blind radio surveys could provide alternative possibilities for exploring DLA galaxies apart from the selection biases in photometric surveys.
5. DLA galaxies display a wide range in SFRs with the mean about $10^{-2} M_{\odot} \text{ yr}^{-1}$. This suggests that DLA galaxies consist of dwarf galaxies in which SFRs are low comparable to those in LSB galaxies.

Although more data would be required to confirm these conclusions, this study suggests that *LSB dwarf galaxies primarily contribute to the population of DLA systems, while massive spiral galaxies, which is less abundant, also should be DLA systems.*

Some previous attempts have been made to detect DLA galaxies much closer to background quasars to unveil the nature of DLA systems. Steidel et al. (1997) studied a DLA system at $z = 0.656$ from photometric images and spectroscopy of the quasar 3C336 field. They concluded that there is no galaxy brighter than $0.05L_K^*$ within 0.5 arcsec, corresponding to a radius $\sim 2h^{-1}$ kpc, to the quasar line of sight. Bouché et al. (2001) tried to detect

H α emission in the region behind the PSF of the same quasar 3C336. But they failed to detect any H α emitters in the vicinity of the line of sight of the quasar with the range from 0.24 to 30 h $^{-1}$ kpc. In this observation, they reported that the 3σ flux limit was $\sim 3 \times 10^{-17}$ h $^{-2}$ ergs s $^{-1}$ cm $^{-2}$ for an unresolved source. This corresponds to an SFR of 0.3 h $^{-2}$ M $_{\odot}$ yr $^{-1}$. Our results show that the mean SFR at $z \sim 0.65$ is $\sim 10^{-2}$ M $_{\odot}$ yr $^{-1}$ which are much lower than the SFR corresponding to the flux limit. Therefore, if LSB galaxies dominate the population of DLA systems, the low surface brightness, corresponding to the low SFR, may prevent us from detecting H α emission.

If a PSF size θ_{th} is constant at $z > 1$, the physical size corresponding to θ_{th} becomes smaller, so that the masking effect would be less serious than the samples at redshifts $z \lesssim 1$. Kulkarni et al. (2000) reported that they were able to detect an H α emission feature from a DLA system at $z = 1.892$ at a projected separation of 0.25 arcsec from a line of sight toward the quasar LBQS 1210+1731, using *HST* NICMOS. They concluded that the size of the H α emitter would be 2 – 3 kpc if it is associated with the DLA system and the feature is not PSF artifacts. Fynbo et al. (1999), Møller et al. (2002), and Møller, Fynbo & Fall (2004) have successfully detected five DLA galaxies at $2 \leq z \leq 3$. They found that all Ly α emitters reside in very close proximity to background-quasar lines of sight, and concluded that they have small impact parameters about 1-3 kpc. Although these are observational properties of high-redshift ($z > 2$) DLA galaxies, it is suggestive to recognize the fact that their conclusions are consistent with our results.

It may be more likely that DLA galaxies can be identified at $z \sim 0$ than high-redshift ones. This is partly because a physical size corresponding to a constant θ becomes small toward present enough to identify compact galaxies around a quasar line of sight, and partly because surface brightnesses of DLA galaxies are expected to be so high as to detect their photometric images. Like a DLA galaxy (SBS1543+593) at $z = 0.009$ (Schulte-Ladbeck et al. 2004), DLA galaxies at $z \sim 0$ have advantages that their detection is less affected by the masking effect and/or their faintness than high-redshift ones because they are close to us. Thus we again emphasize our conclusions that the selection biases are very important to understand the nature of DLA galaxies and to interpret results of photometric observations.

The radio observations offer some possibilities for exploring the nature of H I-rich galaxies such as DLA systems. Some blind 21 cm surveys provide interesting information to establish fundamental properties of local H I-selected galaxies such as the H I mass function, which is the distribution function of galaxies as a function of the H I mass, the relation between the H I mass and the near-IR luminosity of their counterparts, and so on (Zwaan et al. 2003; Rosenberg & Schneider 2003). For example, the H I Parkes All-sky Survey (HIPASS) is an ongoing blind survey which has samples of 1000 galaxies with the H I masses $10^{6.8} \lesssim$

$M_{\text{HI}} \lesssim 10^{10.6} M_{\odot}$ (Zwaan et al. 2003). These samples indicate that the H I-selected galaxies exhibit interesting properties such as the H I mass function. Since the HIPASS samples consist of H I-gas systems with $N_{\text{HI}} \gtrsim 10^{19} \text{ cm}^{-2}$ including sub-DLA systems and Lyman-limit systems, such direct measurements of the H I-gas systems can provide stringent constraints on observations and formation theories of DLA galaxies, sub-DLA systems and faint dwarf galaxies such as LSB galaxies. The studies of the optical counterparts could offer special insights to their nature. Moreover, their natures can be unveiled by investigating the missing link between H I-selected galaxies and optical ones.

We thank N.Gouda, S.Yoshioka, M.Enoki, H.Yahagi and T.Yano for valuable discussions of this study and the anonymous referee for careful reading of this manuscript and suggestions, which improved the clarity of this presentation. K.O. thanks Arthur Wolfe for an interesting suggestion and Kentaro Nagamine for stimulating discussions, particularly for star formation rates in comparison with his numerical results. M.N. also acknowledges a PPARC rolling grant for extragalactic astronomy and cosmology and the Japan Society for the Promotion of Science for Young Scientists (No.207).

REFERENCES

- Bardeen, J. M., Bond, J. R., Kaiser, N. & Szalay, A. S. 1986, *ApJ*, 304, 15
- Bond, J. R., Cole, S., Efstathiou, G., & Kaiser, N. 1991, *ApJ*, 379, 440
- Bouché, N., Lowenthal, J. D., Charlton, J. C., Bershadsky, M. A., Churchill, C. W., & Steidel, C. C. 2001, *ApJ*, 550, 585
- Bower, R. 1991, *MNRAS*, 248, 332
- Bowen, D. V., Tripp, T. M., & Jenkins, E. B. 2001, *AJ*, 121, 1456
- Chen, H-W., & Lanzetta, K. M. 2003, *ApJ*, 597, 706
- Cox, A. N., 2000, *Allen’s Astrophysical Quantities* (4th ed.; New York: AIP, Springer)
- Fynbo, J. P. U., Møller, P., & Warren, S. J. 1999, *MNRAS*, 305, 849
- Kauffmann, G. 1996, *MNRAS*, 281, 475
- Kennicutt, R.C., Jr, 1998, *ARA&A*, 36, 189
- Kodama, T., & Arimoto, N. 1997, *A&A*, 320, 41

- Kulkarni, V. P., Hill, J. M., Schneider, G., Weymann, R. J., Storrie-Lombardi, L. J., Rieke, M. J., Thompson, R. I., & Jannuzi, B. T. 2000, *ApJ*, 536, 36
- Lacey, C. G., & Cole, S. 1993, *MNRAS*, 262, 272
- Le Brun, V., Bergeron, J., Boissé, P., & Deharveng, J. M., 1997, *A&A*, 321, 733
- Maller, A. H., Prochaska, J. X., Somerville, R. S., & Primack, J. R. 2001, *MNRAS*, 326, 1475
- Maller, A. H., Prochaska, J. X., Somerville, R. S., & Primack, J. R. 2001, *MNRAS*, 343, 268
- McKee, C. F., & Ostriker, J. P. 1977, *ApJ*, 218, 148
- Møller, P., Warren, S. J., Fall, S. M., Fynbo, J. P. U., & Jakobsen, P. 2002, *ApJ*, 574, 51
- Møller, P., Fynbo, J. P. U., & Fall, S. M. 2004, *A&A*, 422, L33
- Nagamine, K., Springel, V., & Hernquist, L. 2004, *MNRAS*, 348, 435
- Nagashima, M., Totani, T., Gouda, N., & Yoshii, Y. 2001, *ApJ*, 557, 505 (NTGY)
- Okoshi, K., Nagashima, M., Gouda, N., & Yoshioka S., 2004, *ApJ*, 603, 12 (Paper I)
- Osterbrock 1989, *Astrophysics of Gaseous Nebulae and Active Galactic Nuclei*, University Science Books
- Péroux, C., McMahon, R. G., Storrie-Lombardi, L. J., & Irwin, M. J. 2003, *AJ*, 346, 1103
- Petrosian, A. R., Boulesteix, J., Comte, G., Kunth, D., & Leoarer, E. 1997, *A&A*, 318, 390
- Press, W., & Schechter, P. 1974, *ApJ*, 187, 425
- Prochaska, J. X., Gawiser, E., Wolfe, A. M., Castro, S. & Djorgovski, S. G. 2003, *ApJL*, 595, L9
- Prochaska, J. X., & Herbert-Fort, S. 2004, *PASP*, 116, 622
- Prochaska, J. X., & Wolfe, A. M. 1996, *ApJ*, 470, 403
- Somerville, R. S., & Kolatt, T. 1999, *MNRAS*, 305, 1
- Somerville, R. S., Primack, J. R., & Faber, S. M. 2001, *MNRAS*, 320, 504
- Rao, S. M., Nestor, D.B., Turnshek, D. A., Lane, W. M., Monier E. M., & Bergeron, J. 2003, *ApJ*, 595, 94

- Rao, S. M., & Turnshek, D. A. 1998, *ApJ*, 500, L115
- Rao, S. M., & Turnshek, D. A. 2000, *ApJS*, 130, 1
- Rosenberg, J. L., & Schneider, S. E. 2003, *ApJ*, 585, 256
- Schulte-Ladbeck, R. E., Rao, S. M., Drozdovsky, I. O., Turnshek, D. A., Nestor, D. B., & Pettini, M. 2004, *ApJ*, 600, 613
- Steidel, C. C., Dickinson, M., Meyer, D. M., Adelberger, K. L., & Sembach, K. R. 1997, *ApJ*, 480, 568
- Steidel, C. C., Pettini, M., & Persson, S. E. 1994, *AJ*, 108, 2046
- Storrie-Lombardi, L. J., & Wolfe, A. M. 2000, *ApJ*, 543, 552
- van den Hoek, L. B., de Blok, W. J. G., van der Hulst, J. M., & de Jong, T. 2000, *A&A*, 357, 397
- van Zee, L. 2001, *AJ*, 121, 2003
- Vladilo, G., Centuri3n, M., Bonifacio, P., & Howk, J. C. 2001, *ApJ*, 557, 1007
- Warren, S. J., M3ller, P., Fall, S. M., & Jakobsen, P. 2001, *MNRAS*, 326, 759
- Wolfe, A. M., Turnshek, D. A., Smith, H. E., & Cohen, R. D. 1986, *ApJS*, 61, 249
- Wolfe, A. M., Prochaska, J. X., & Gawiser E. 2003a, *ApJ*, 593, 215
- Wolfe, A. M., Prochaska, J. X., & Gawiser E. 2003a, *ApJ*, 593, 235
- Wolfire, M. G., Hollenbach, D., McKee, C. F., Tielens, A. G. G. M., & Bakes, E. L. 1995, *ApJ*, 443, 152
- Zwaan, M. A. et al. 2003, *ApJS*, 125, 2842

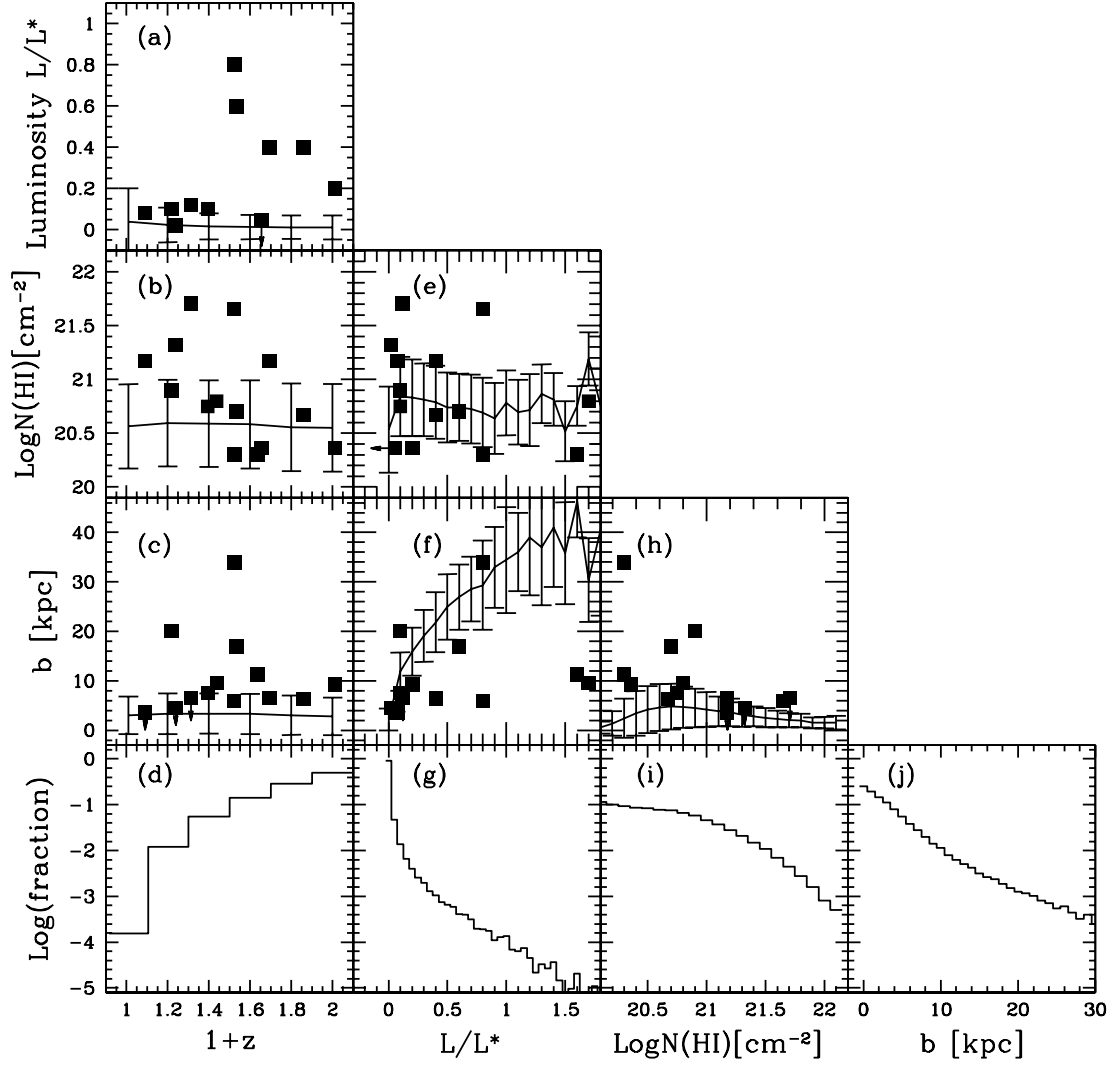


Fig. 1.— Fundamental properties of DLA galaxies at redshifts $0 \leq z \leq 1$. Error bars with the averages indicate 1σ errors. The square symbols are the observational data (Rao et al. 2003). B-band luminosities are plotted in figures but two data for which the luminosities are measured in K-band only. The data with an upper limit of the luminosity are the DLA system in the 3C336 quasar field. More information for detail is presented in Rao et al. (2003). Note that the number fraction is ~ 0.98 ($L \leq 0.1L^*$) in panel(g).

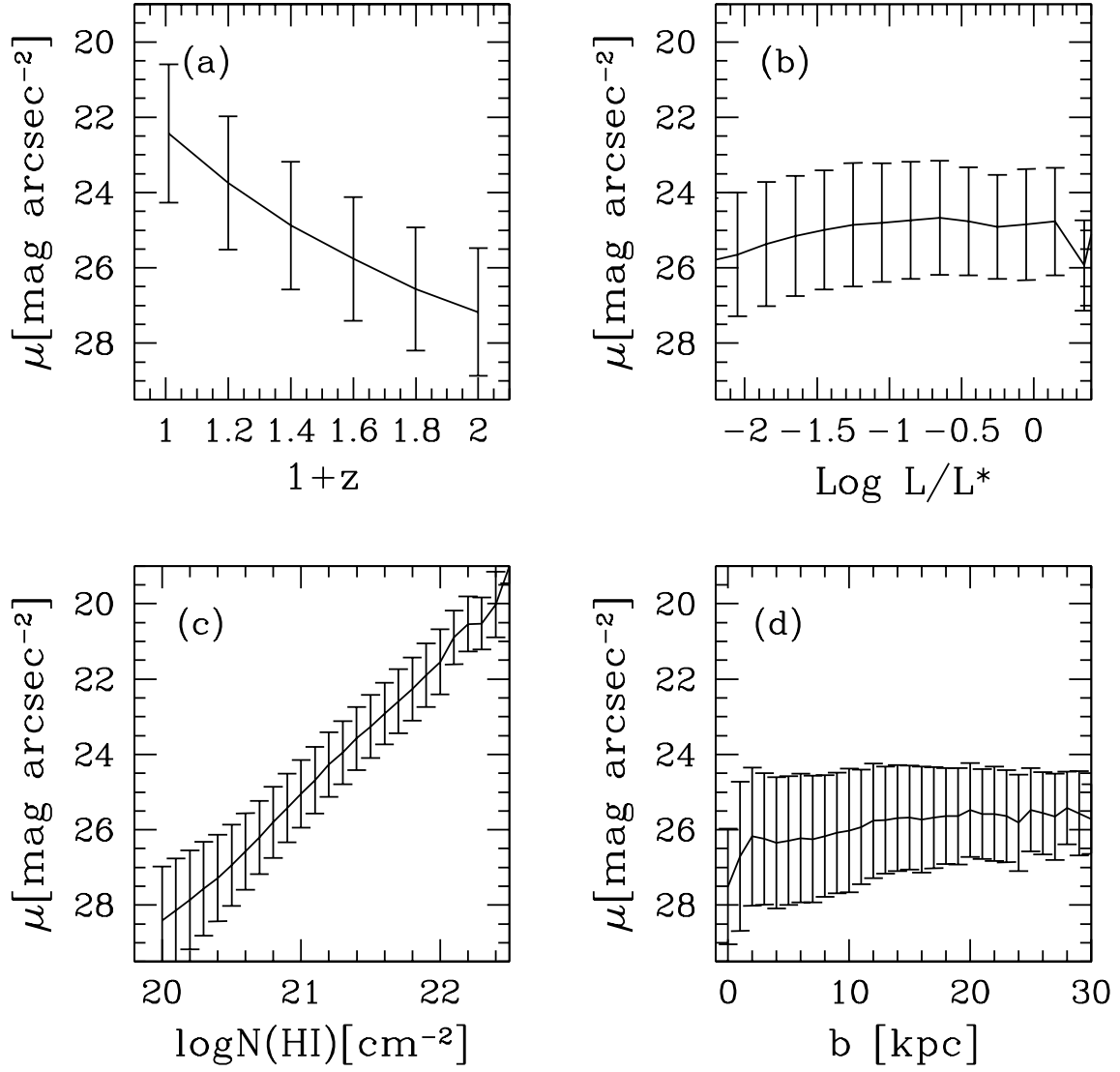


Fig. 2.— Central surfaceness brightness μ in B-band of DLA galaxies as a function of (a) redshift, (b) luminosity, (c) column density and (d) size, respectively. Error bars with the averages indicate 1σ errors.

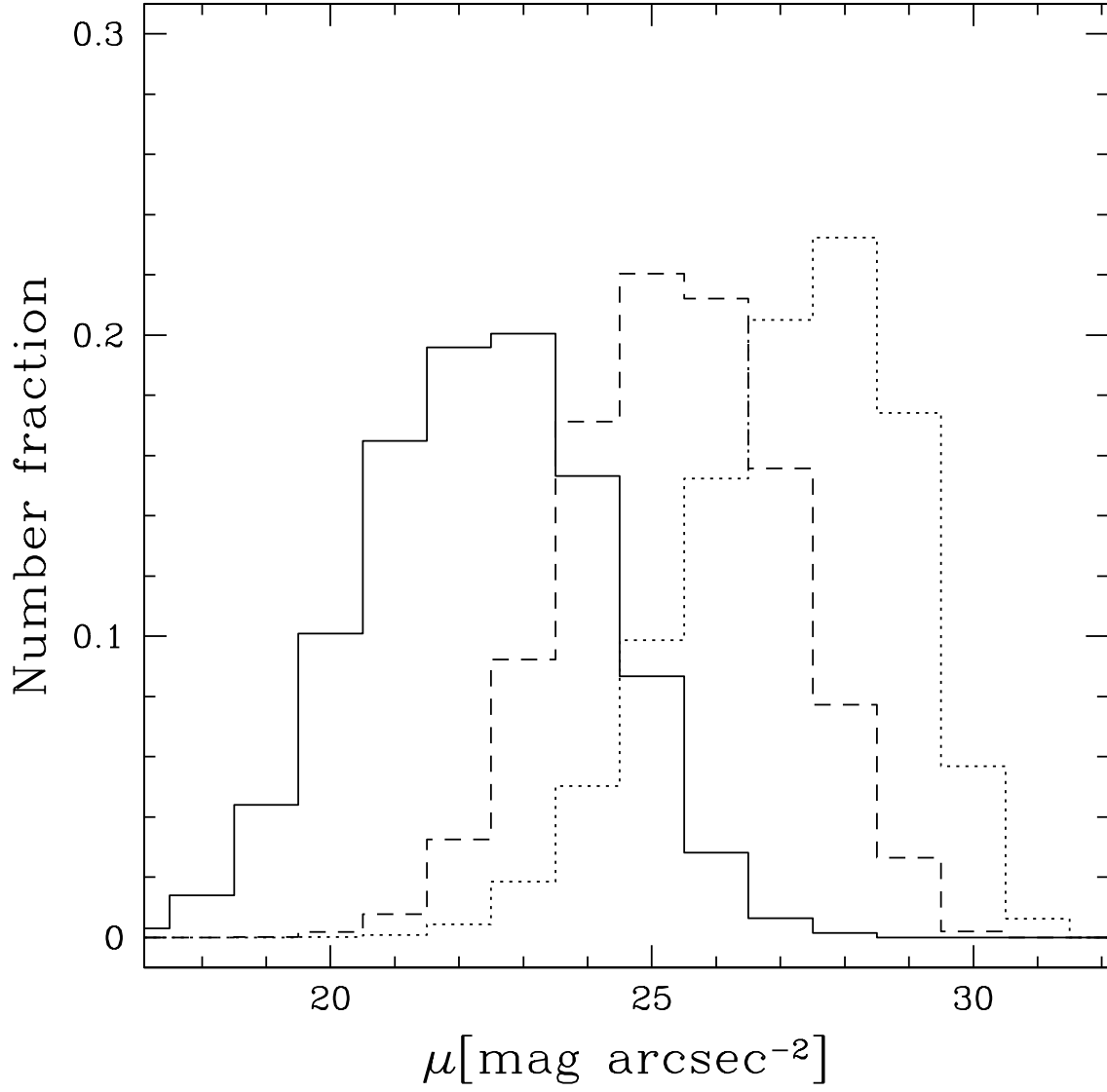


Fig. 3.— Number fractions of DLA galaxies as a function of surface brightness μ in B-band at redshifts $z = 0$ (solid line), 0.5 (dashed line) and 1 (dotted line).

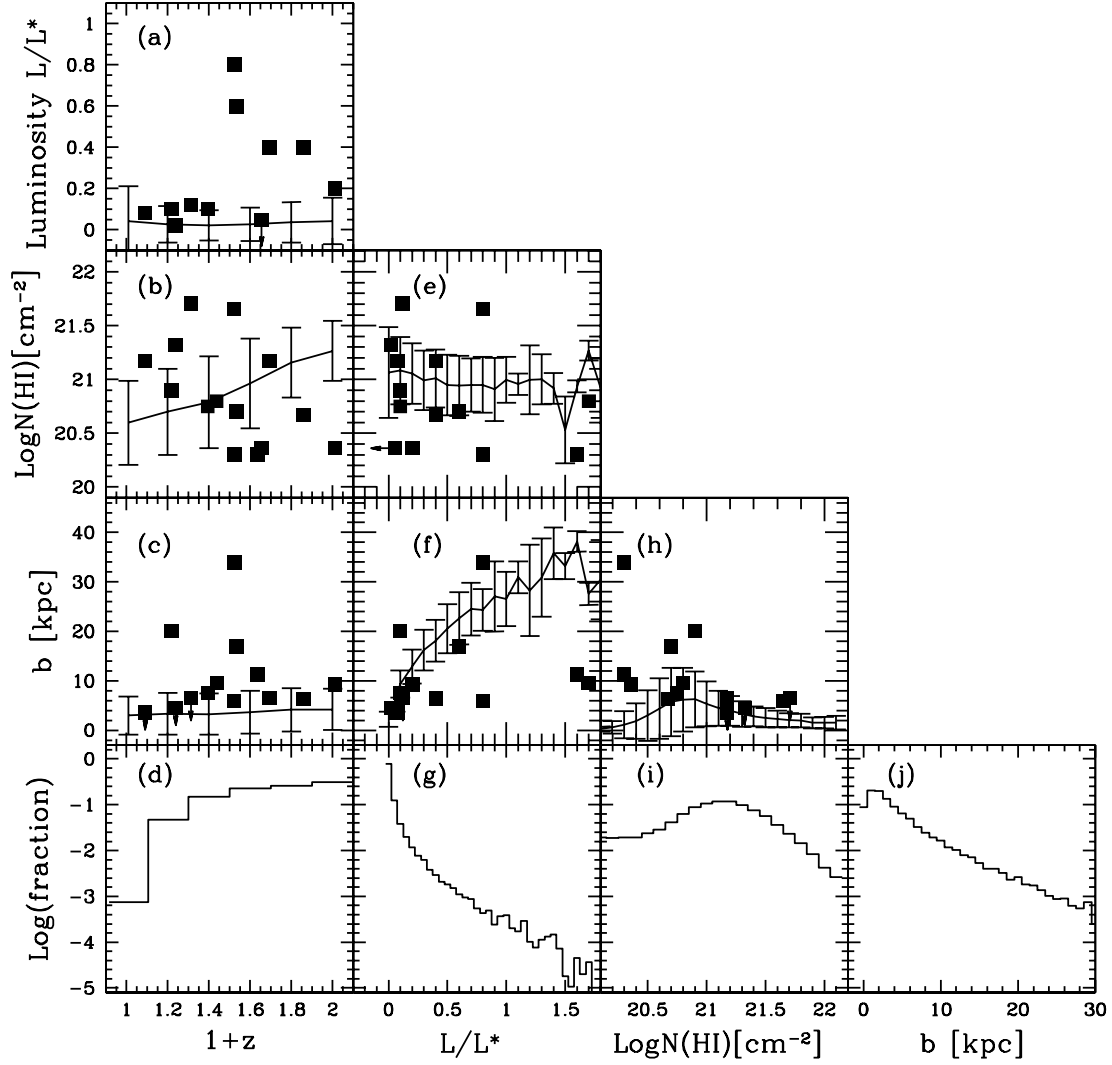


Fig. 4.— Fundamental properties of DLA galaxies at redshifts $0 \leq z \leq 1$ if the central surface brightness $\mu < 25$ [mag arcsec $^{-2}$]. Error bars with the averages indicate 1σ errors. The square symbols are the observational data (Rao et al. 2003). The number fractions in panels (d),(g),(i) and (j) are defined as the ratios the number of DLA galaxies per bin to that of DLA galaxies which fulfill the selection criteria. Note that the number fraction is ~ 0.94 ($L \leq 0.1L^*$) in panel(g).

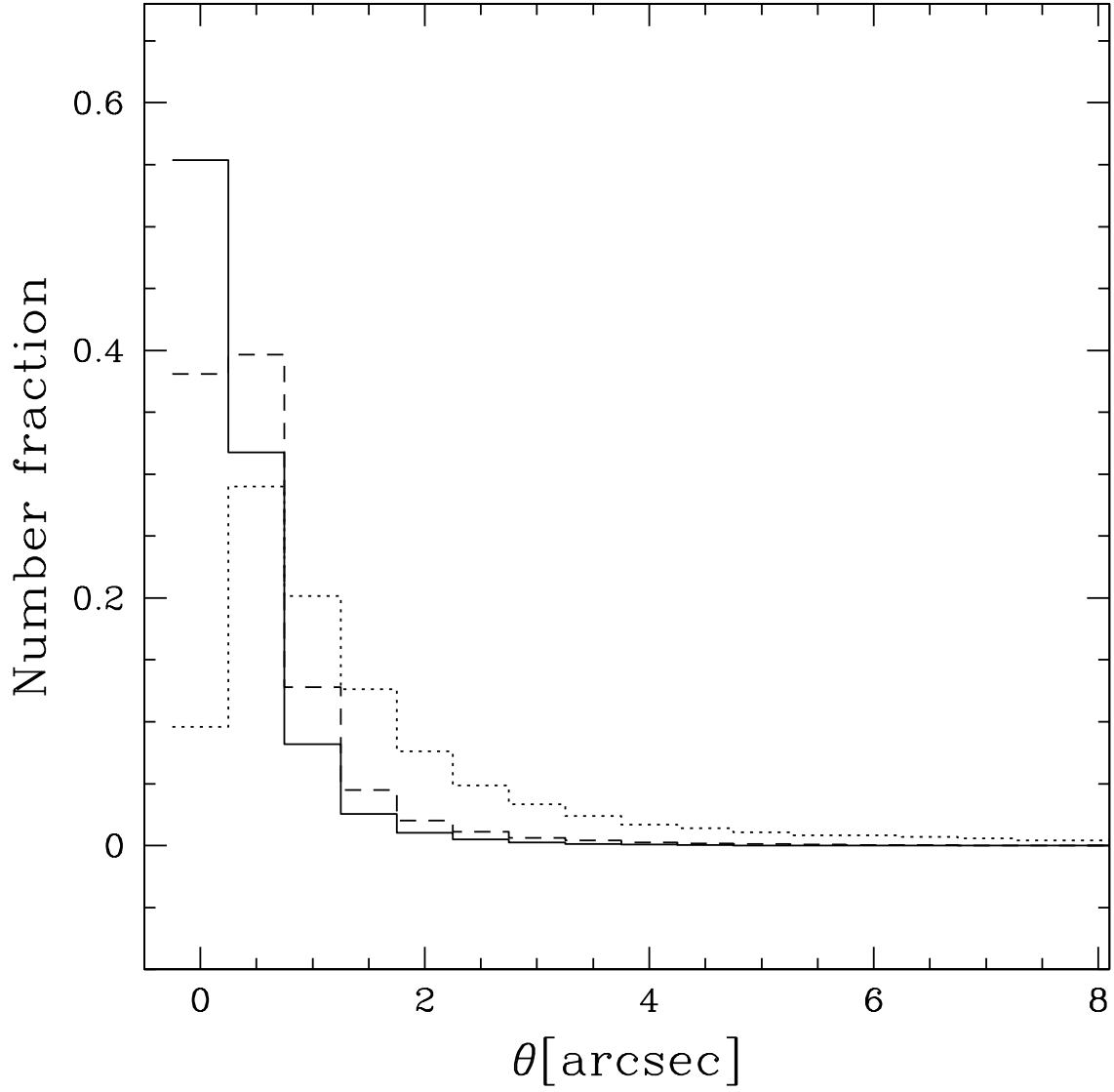


Fig. 5.— Number fractions of DLA galaxies as a function of angular size θ [arcsec] at $z = 0.1$ (dotted line), 0.5 (dashed line) and 1 (solid line).

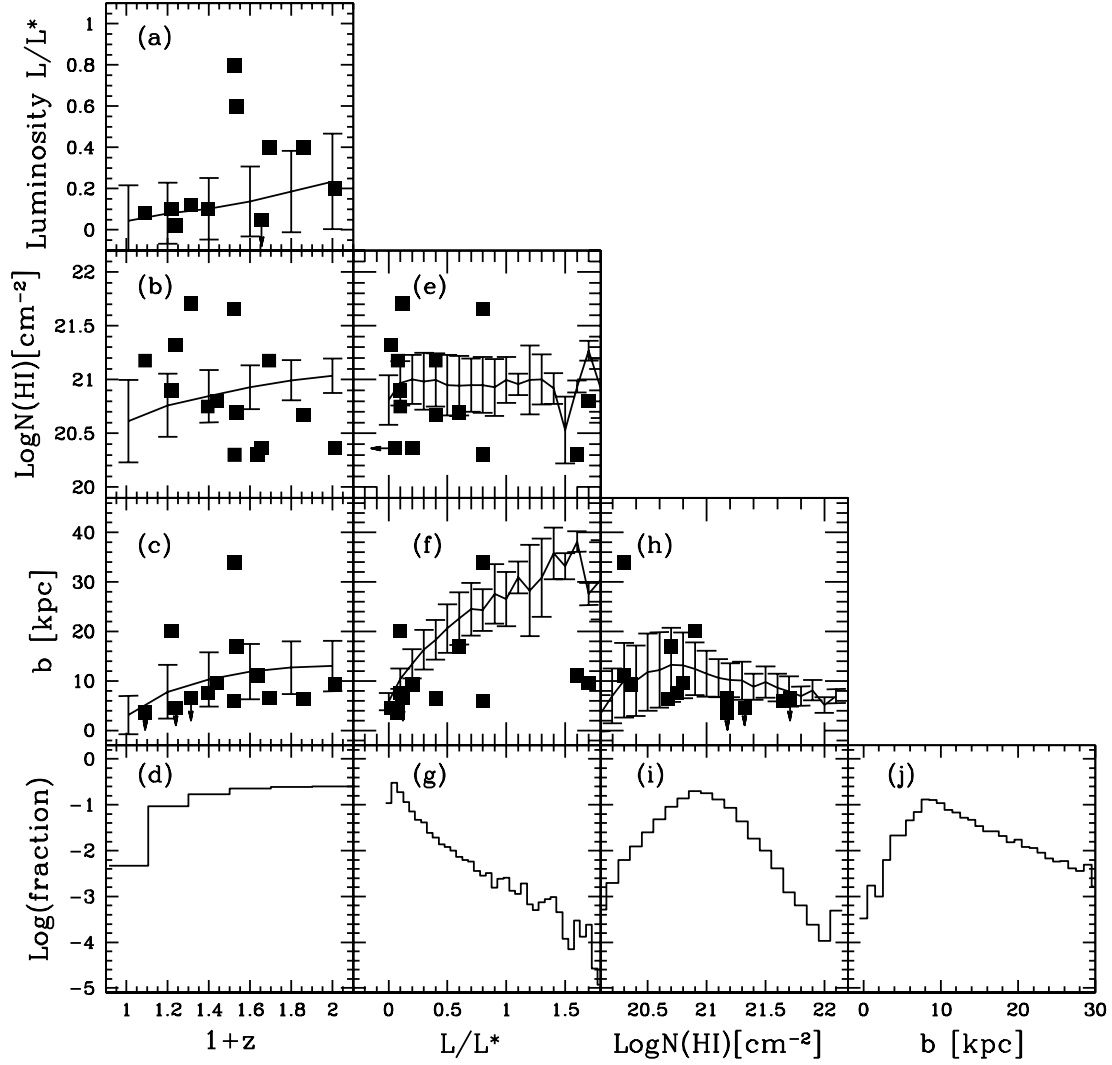


Fig. 6.— Fundamental properties of DLA galaxies at redshifts $0 \leq z \leq 1$ if the angular size $\theta > 1$ [arcsec] in addition to the surface brightness limit $\mu_{\text{th}} = 25$ [mag arcsec $^{-2}$]. Error bars with the averages indicate 1σ errors. The number fractions in panels (d),(g),(i) and (j) are defined as in Figure 4. The square symbols are the observational data (Rao et al. 2003). Note that the number fraction is ~ 0.60 ($L \leq 0.1L^*$) in panel(g).

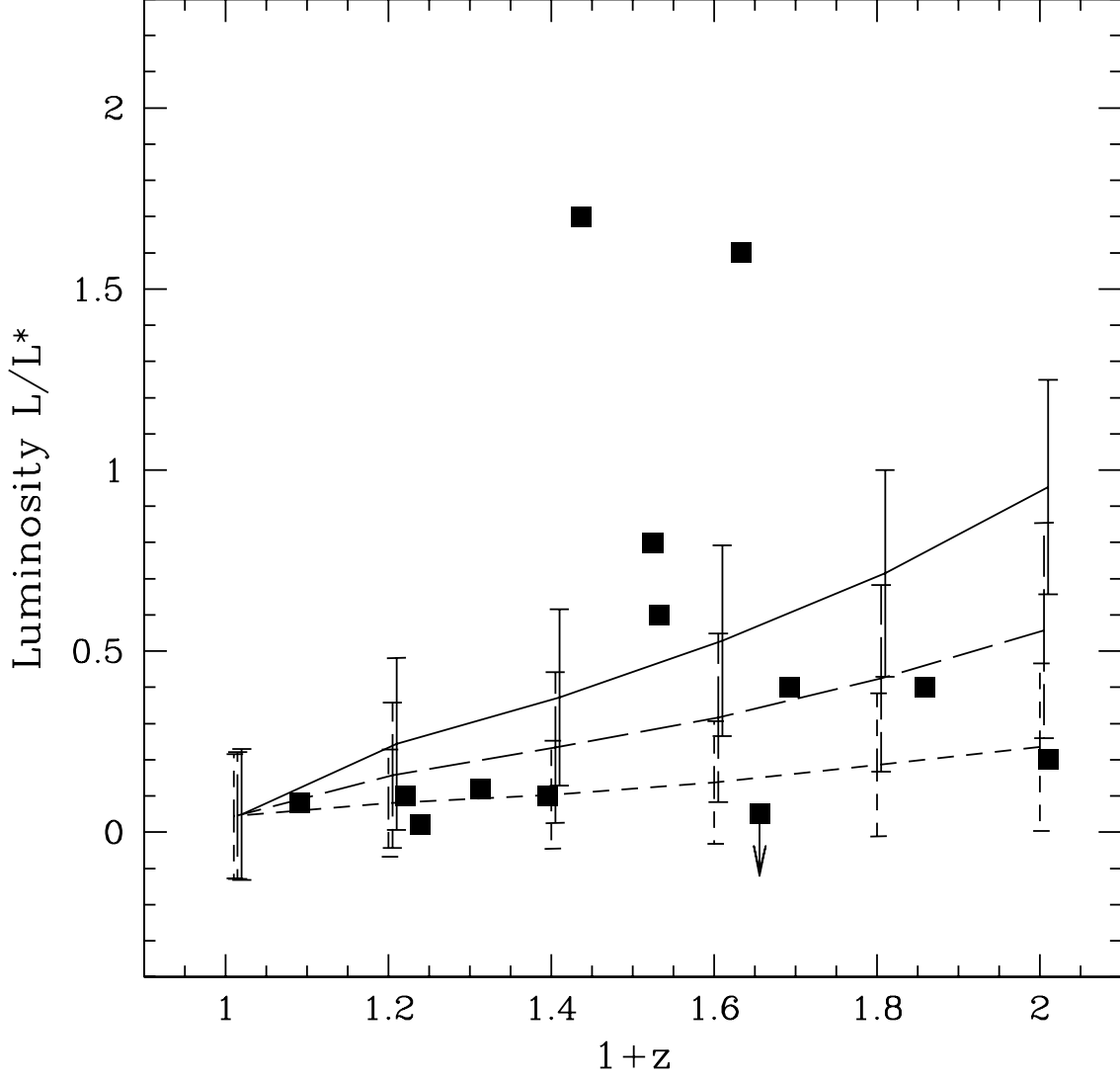


Fig. 7.— Luminosity evolution of DLA galaxies taking into account angular-size limitations: $\theta_{th}=1$ (short-dashed line), 2 (long-dashed line) and 3 (solid line)[arcsec] in addition to the surface brightness limit $\mu_{th} = 25$ [mag arcsec $^{-2}$]. Error bars with the averages indicate 1σ errors. The square symbols are the observational data (Rao et al. 2003).

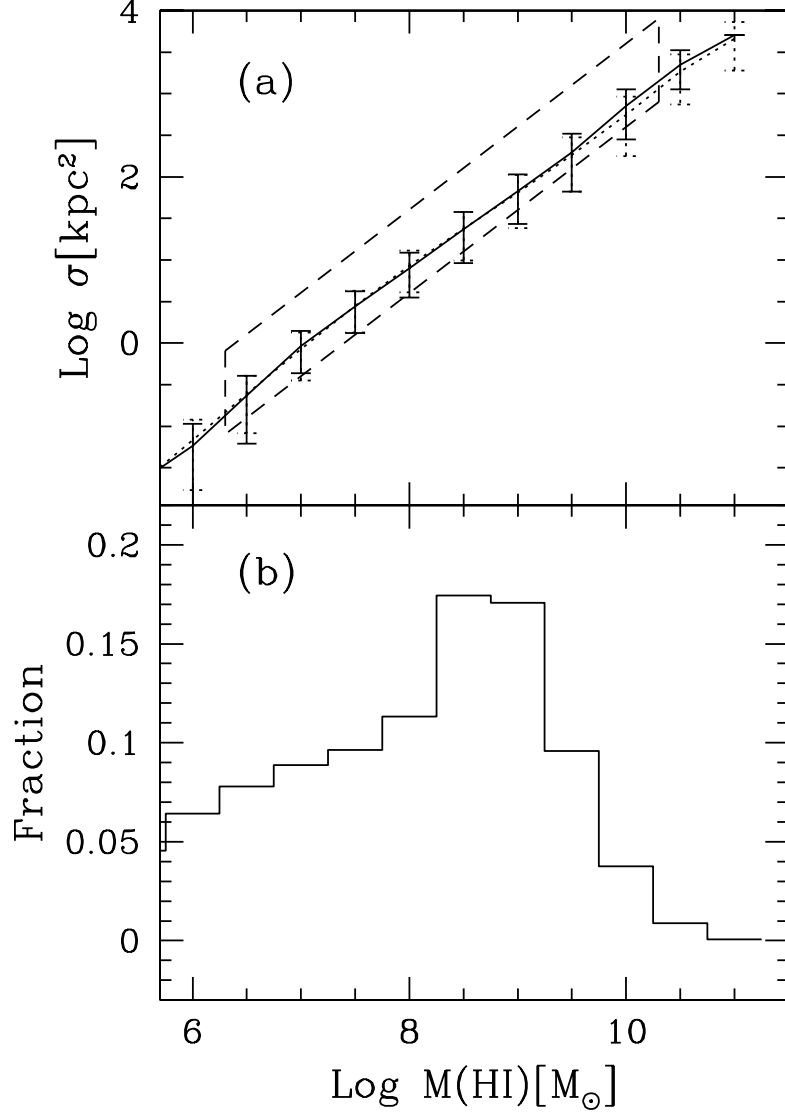


Fig. 8.— Relations with H I mass of DLA galaxies at $0 \leq z \leq 1$. (a) The cross section vs H I mass. The average cross sections at $z = 0$ are plotted as the solid line. Error bars with the averages indicate 1σ errors. The boxes enclosed by dashed lines represent ranges of the observational data from blind 21 cm surveys (Rosenberg & Schneider 2003). We also show the averaged cross-section at $0 \leq z \leq 1$ as the dotted line which is almost identical with the relation at $z = 0$ (solid line). (b) Number fraction of DLA galaxies as a function of H I mass at $0 \leq z \leq 1$.

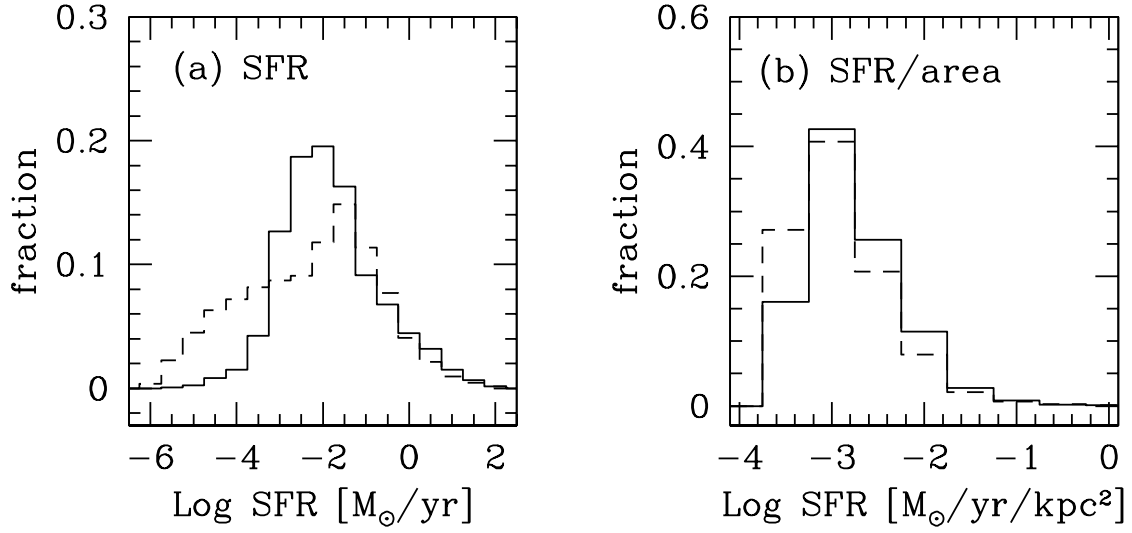


Fig. 9.— (a) Number fractions of DLA galaxies as a function of star formation rate [$M_{\odot} \text{ yr}^{-1}$] at $z = 0$ (solid line) and $z = 1$ (dashed line), respectively. (b) Number fractions as a function of star formation rate per unit area [$M_{\odot} \text{ yr}^{-1} \text{ kpc}^{-2}$] are also shown at $z = 0$ (solid line) and $z = 1$ (dashed line), respectively.

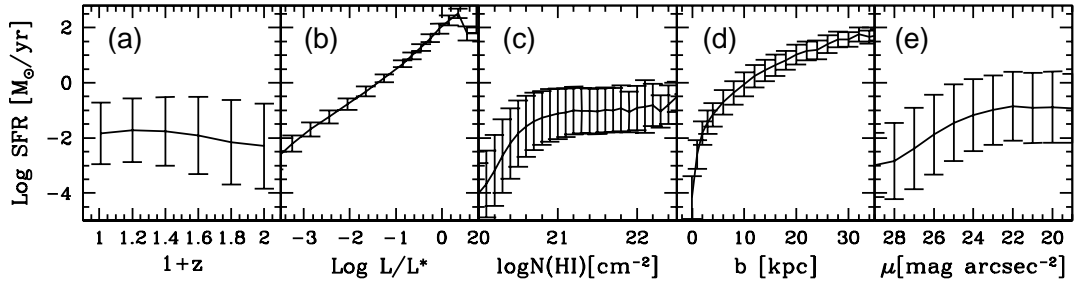


Fig. 10.— Star formation rates of DLA galaxies as a function of (a) redshift, (b) absolute luminosity in B-band, (c) H I column density, (d) size and (e) surface brightness in B-band, respectively. Error bars with the averages indicate 1σ errors.

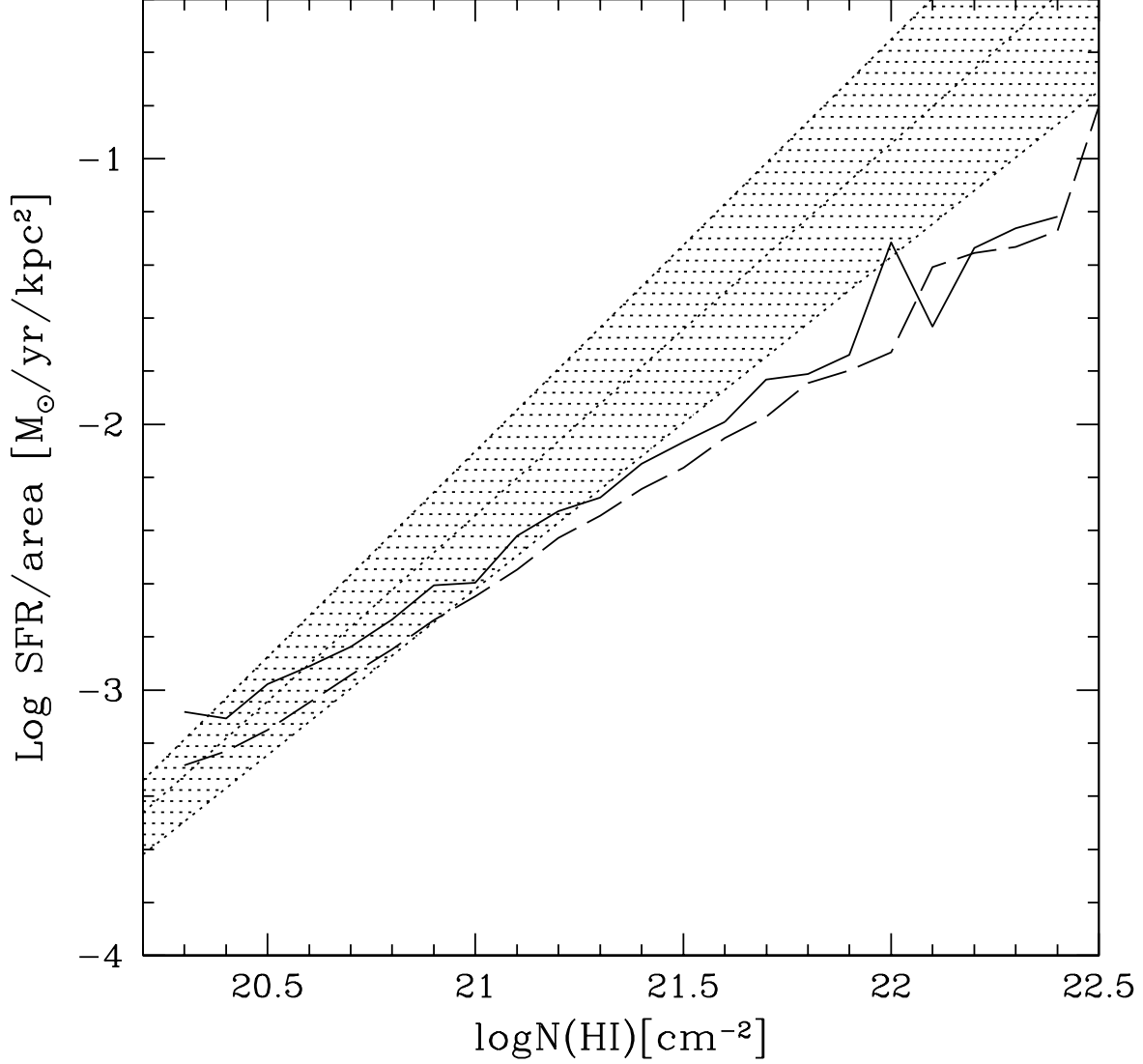


Fig. 11.— Star formation rates per unit area of DLA galaxies as a function of H I column density at redshift $z = 0$ (solid line) and $z = 1$ (long-dashed line) in comparison with the Kennicutt law (1998), respectively. The shaded area indicates the region of SFRs given by equation(3) which includes systematic errors in the SFRs.

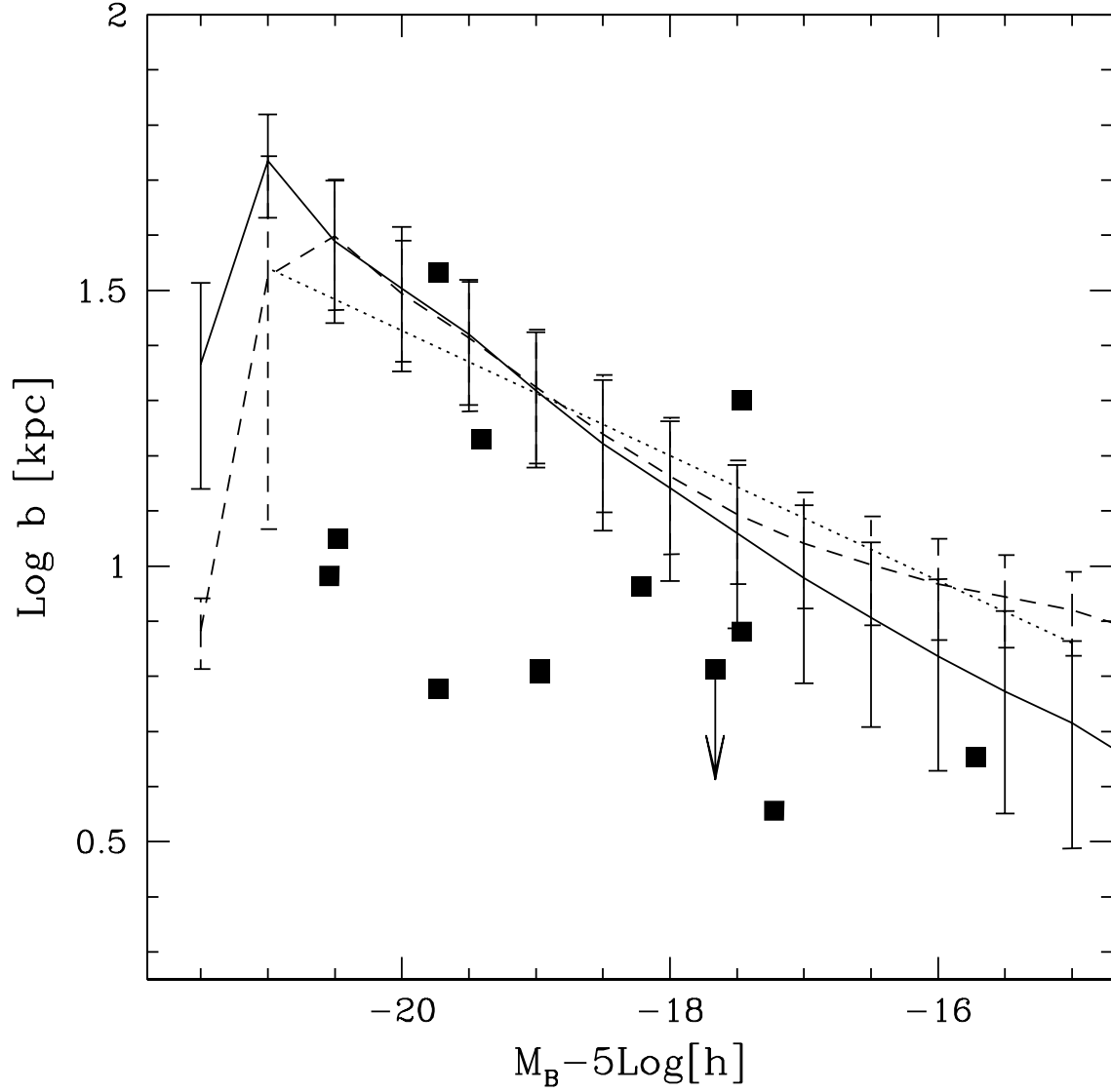


Fig. 12.— The radial size as a function of B-band absolute magnitude: no angular size limitation (solid line) and $\theta > 1$ [arcsec] (dashed line), respectively. As shown in Figure 1, the square symbols are the observational data (Rao et al. 2003). Dotted line shows the scaling relation between magnitudes and H I sizes provided by Chen & Lanzetta (2003). Error bars with the averages indicate 1σ errors.

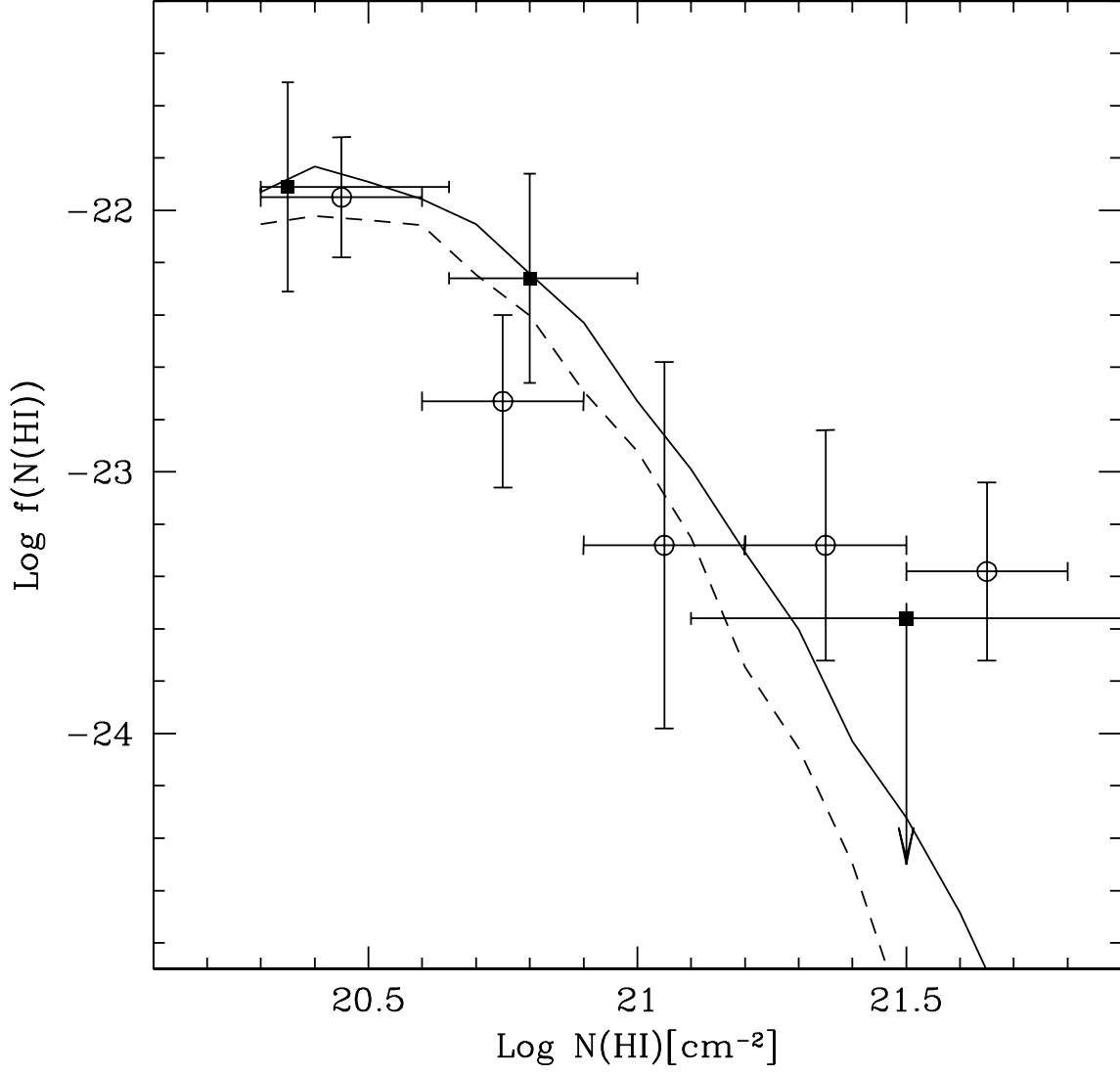


Fig. 13.— H I column density distribution $f(N_{\text{HI}})$ of DLA galaxies at $z = 1$ without selection bias (solid line). We also show $f(N_{\text{HI}})$ with the selection effect caused by the limitation of angular size $\theta_{\text{th}} = 1$ [arcsec] (dashed line). The square symbols with crosses are the observed data shown (Storrie-Lombardi & Wolfe 2000) (closed square). Also shown for another observation at $\langle z \rangle = 0.78$ (Rao & Turnshek 2000) (open circle).